HHS Public Access

Author manuscript

ACS Infect Dis. Author manuscript; available in PMC 2019 November 09.

Published in final edited form as:

ACS Infect Dis. 2018 November 09; 4(11): 1564–1573. doi:10.1021/acsinfecdis.8b00125.

Rapid Uptake and Photodynamic Inactivation of Staphylococci by Ga(III)-Protoporphyrin IX

Ana V. Morales-de-Echegaray[1], **Thora R. Maltais**[1], **Lu Lin**[1], **Waleed Younis**[2], **Naveen R. Kadasala**[1], **Mohamed N. Seleem**[2], **Alexander Wei**[1,*]

[1]Department of Chemistry, Purdue University, 560 Oval Drive, West Lafayette, Indiana, 47907-2084, USA

[2]Department of Comparative Pathobiology, Purdue University, 625 Harrison Street, West Lafayette, IN 47907-2027, USA

Abstract

Antimicrobial photodynamic therapy (aPDT) is a promising method for the topical treatment of drug-resistant staphylococcal infections, and can be further improved by identifying mechanisms that increase the specificity of photosensitizer uptake by bacteria. Here we show that Ga(III)-protoporphyrin IX chloride (Ga-PpIX), a fluorescent hemin analog with previously undisclosed photosensitizing properties, can be taken up within seconds by *Staphylococcus aureus* including multidrug-resistant strains such as MRSA. The uptake of Ga-PpIX by staphylococci is likely diffusion-limited and is attributed to the expression of high-affinity cell-surface hemin receptors (CSHRs), namely iron-regulated surface determinant (Isd) proteins. A structure–activity study reveals the ionic character of both the heme center and propionyl groups to be important for uptake specificity. Ga-PpIX was evaluated as a photosensitizer against *S. aureus* and several clinical isolates of MRSA using a visible light source, with antimicrobial activity (3-log reduction in CFU/mL) at 0.03 μM with 10 seconds of irradiation by a 405-nm diode array (1.4 J/cm^2); antimicrobial activity could also be achieved within minutes using a compact fluorescent lightbulb. GaPpIX was many times more potent than PpIX, a standard photosensitizer featured in clinical aPDI, but also demonstrated low cytotoxicity against HEK293 cells and human keratinocytes. Ga-PpIX uptake was screened against a diverse panel of bacterial pathogens using a fluorescence-based imaging assay, which revealed rapid uptake by several Gram-positive species known to express CSHRs, suggesting future candidates for targeted aPDT.

Graphical Abstract

*To whom correspondence should be addressed. alexwei@purdue.edu.

Supporting Information. Data from photophysical measurements of Ga-PpIX; microbiological culture conditions; details of fluorescence imaging and analysis; data from competitive uptake assays; details on LED and CFL sources; additional data from aPDI studies using CFL source; *t*-tests for cytotoxicity assays; synthesis and ^{1}H NMR spectra of PpIX derivatives **1**, **2**, **6**, **11**, and **12**. This material is available free of charge via the Internet at http://pubs.acs.org.

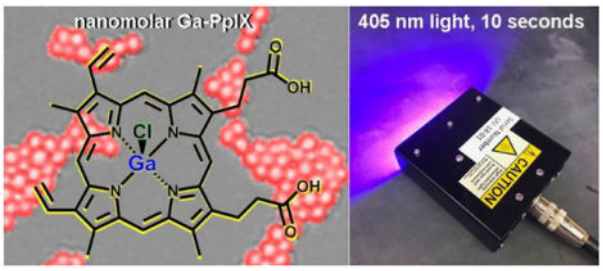

Keywords

Staphylococci; MRSA; photodynamic therapy; hemin; porphyrins; targeted delivery

Staphylococcus aureus and its multidrug-resistant (MDR) strains remain the leading cause of hospital-associated infections, despite attempts to address this problem over the last several decades.[1,2,3] Vancomycin, the current gold standard for combating methicillin-resistant *S. aureus* (MRSA), is compromised by the rise of vancomycin-resistant strains, and while newer drugs such as linezolid and daptomycin have been recommended as alternatives,[4] MRSA strains with demonstrated resistance against these have already emerged.[5,6] In fact, the speed with which *S. aureus* and other pathogens can develop or acquire antibiotic resistance threatens to jeopardize any therapy that relies on conventional drug paradigms.[7]

A possible exception to this argument is antimicrobial photodynamic therapy (aPDT), in which a photosensitizer is delivered to microbial pathogens for generating singlet oxygen and other reactive oxygen species (ROS) upon irradiation with light.[8,9] aPDT cannot be easily overcome by established mechanisms of antibiotic resistance,[10] and has been found to be particularly effective against Gram-positive MDR bacteria such as MRSA.[11] aPDT can be applied in situations that are not limited by light penetration into tissue, and has been found to be compatible with keratinocytes;[12] established clinical aPDT examples include the topical treatment of acne[13,14] and the decolonization of bacteria in oral cavities (periodontal disease).[15,16] Ongoing clinical trials and *in vivo* studies indicate that aPDT should also be effective for disinfection of open wounds,[17,18,19] and decolonization of exposed skin prior to surgery to mitigate post-operative infections.[20]

Topically administered aPDT holds great promise to reduce or prevent MRSA infections, but the efficient delivery and selective uptake of photosensitizers should also be considered.[17,18] For example, many photosensitizers are cationic or hydrophobic in nature, resulting in their indiscriminate uptake into mammalian cells as well as bacteria. This not only contributes toward collateral cytotoxicity, but also reduces the amount of available photosensitizer for aPDT. Such issues are being addressed by developing photosensitizer conjugates for their targeted delivery to bacteria.[21] Molecular uptake pathways associated with bacterial virulence are especially attractive in this regard, although incorporation of a targeting ligand may result in added complexity.

Hemin acquisition systems offer natural portals for the bacterial uptake of photosensitizers, and obviate the need to design synthetic conjugates. Although hemin itself (Fe(III)-

protoporphyrin IX chloride, or Fe-PpIX) does not have photosensitizing properties, deferrated species such as PpIX and hematoporphyrin (HP) are highly photoactive and have been widely used in aPDT.[22,23] Non-iron metalloporphyrins are also good candidates for uptake by hemin acquisition systems, many of which are chemically more robust than their unmetallated forms.[24,25,26,27] Seminal work by Stojiljkovic has shown that non-iron PpIX species are readily taken up by bacterial hemin uptake pathways, and also exhibit low collateral toxicity in human cell lines and in rodent models.[28] Non-iron PpIX species have been investigated as antimicrobial agents[28,28,29,30,31] but remarkably their utility for aPDT remains to be explored,[32] despite the long history of porphyrin-based photosensitizers in photodynamic therapies.

In this work we show that Ga(III)-protoporphyrin IX chloride (Ga-PpIX), a fluorescent analog of hemin, exerts an antimicrobial effect against *S. aureus* and several clinical isolates of MRSA at nanomolar concentrations, following a 10-second exposure to a visible light source array operating at 405 nm. The uptake of Ga-PpIX by *S. aureus* is faster than our ability to measure experimentally, and appears to be diffusion-controlled. The primary mechanism of Ga-PpIX uptake involves cell-surface hemin receptors (CSHRs), most likely the iron-regulated surface determinant (Isd) proteins in the case of *S. aureus*,[33,34] which can be exploited for targeted delivery. Structure–uptake studies using various PpIX derivatives reveal important features for rapid and specific uptake by this pathway. We also show that Ga-PpIX is superior in potency to several other photosensitizers, yet has low dark cytotoxicity to human kidney cells and keratinocytes, as well as negligible phototoxicity to the latter under aPDT conditions. Lastly, we establish the importance of CSHRs for targeted Ga-PpIX uptake by screening a wider panel of Gram-positive and -negative bacteria having diverse hemin acquisition systems, and identify several other pathogens as candidates for rapid aPDT.

Results and Discussion

Photophysical properties of Ga-PpIX.

Absorption spectroscopy of PpIX (prepared by deferration of hemin chloride with iron powder) and Ga-PpIX (prepared by microwave heating with anhydrous $GaCl_3$) reveals a distinct change in the Q bands (475–650 nm) characteristic of metal substitution, but a modest narrowing of the Soret band at 405 nm (Figure 1).[26] Fluorescence spectroscopy reveals a blueshift in the emission band of Ga-PpIX of over 80 nm, with a primary emission band at 575 nm and secondary emission at 628 nm. The fluorescence quantum yield of Ga-PpIX at 405 nm is 6.3%, which is sufficient for quantitative image analysis of bacterial labelling or uptake. The singlet-oxygen quantum yield (ϕ_Δ) of Ga-PpIX was estimated by the electron paramagnetic resonance (EPR)-based method described by Nakamura *et al*,[35] using a 405-nm light-emitting diode (LED) array for excitation and tetrakis(1-methyl-4-pyridinio)porphyrin (TMPyP) as a reference compound (ϕ_Δ in water: 77%).[36] Standard curves of EPR signal intensities yield a ϕ_Δ of 45% (Figure S2, Supporting Information).

Bacterial uptake of Ga-PpIX.

In a previous study on the bacterial recognition of hemin, we found *S. aureus* to be especially avid in its binding of hemin conjugates with observable adhesion on the order of minutes, leading us to postulate the role of high-affinity CSHRs (specifically Isd proteins) in rapid hemin uptake.[37] Isd expression is well known to be activated by the ferric uptake regulator (*fur*) gene, and increases upon iron deprivation.[33,38] This led us to compare Ga-PpIX uptake by *S. aureus* cultured in standard and iron-limited conditions, with modest levels observed by the former but dramatically higher uptake by the latter, corresponding with greater avidity (Figure S4, Supporting Information). Iron-deficient conditions are relevant from a clinical perspective, as the body withdraws all available sources of iron during infection, inducing pathogens to express various iron acquisition systems including CSHRs.

In this study, Ga-PpIX was deployed as a fluorescent hemin analog to characterize its rate of uptake by *S. aureus* using flow cytometry. Suspensions of *S. aureus* (PC 1203) cultured in iron-deficient media were rapidly mixed with Ga-PpIX in phosphate buffered saline (PBS), incubated at room temperature for fixed intervals between 10 seconds and 40 minutes, then fixed with 4% paraformaldehyde and subjected to flow cytometry. Remarkably, only minor variations in fluorescence were observed, regardless of exposure times to Ga-PpIX (Figure 2). The absence of a fluorescence buildup period over time implies that the capture of Ga-PpIX by CSHRs is likely diffusion-controlled.

While the rapid bacterial uptake of Ga-PpIX is of primary interest, we considered whether Ga-PpIX accumulation might be affected adversely by the activation of bacterial efflux pumps, a known mechanism for removing excessive hemin to prevent acute iron toxicity.[39] In this study, we did not obtain conclusive evidence of Ga-PpIX-activated efflux, relative to the timescale of photodynamic inactivation (see below). Given our observation of rapid Ga-PpIX uptake, we reasoned that maximum aPDT efficacy could be achieved by applying light irradiation immediately after introducing Ga-PpIX, and would also circumvent hemin efflux as a potential resistance mechanism.

To elucidate the most relevant structural features for Ga-PpIX uptake by *S. aureus*, we performed a competitive uptake assay using one equivalent of hemin against Ga-PpIX (**1**), PpIX (**2**), and eleven other fluorescent porphyrin derivatives, with evaluation by fluorescence imaging after 15 minutes of co-incubation (Figure 3 and Table S1, Supporting Information). These studies were guided in part by insights taken from the X-ray structures of hemin and Ga-PpIX within the binding pocket of IsdH:[40] (i) apical coordination of the trivalent metal center by a tyrosine residue; (ii) flanking of the vinyl groups on pyrrole rings A and B by nearby aromatic residues; and (iii) the extension and presumed hydration of the propionyl groups (rings C and D) outside of the binding pocket.

The competitive uptake assay produced three important observations: (i) the uptake of Ga(III)-PpIX (**1**) was strongly affected by competition with hemin chloride, with greater than 80% reduction in fluorescence versus the positive control without hemin; (ii) the uptake of diacids PpIX (**2**), Zn(II)-PpIX (**3**), HP (**4**), and Zn(II)-HP (**5**) were moderately affected by hemin; and (iii) uptake of dimethyl diesters **6–8** (derived from **1**, **2**, and **4**), tetraesters **9** and

10 (di-*O*-acetyl and -succinyl derivatives of **8**), diacetyldeuteroporphyrins (DiAcDP) **11** and **12**, and verteporfin **13** were all less affected by hemin relative to their diacid counterparts, indicating nonspecific uptake as a major or dominant mechanism.

The competitive uptake of **1** (in red) versus compounds **2–5** (in blue) suggests that the CSHRs on *S. aureus* have stronger affinity for ionic heme groups (with trivalent metal ions) and weaker affinity for neutral ones, with nonspecific uptake pathways gaining significance in the latter case. Replacement of carboxylic acids with non-ionizable esters (compounds **6–13**) resulted in further loss of selective uptake, to the extent that CSHR expression no longer played a major role. These observations were confirmed by control experiments using *S. aureus* cultured in standard (iron-replete) media, with a large decrease in the uptake efficiency of **1** and a moderate decrease in the case of **2**, but with little or no effect for several diester derivatives, indicating uptake of the latter to be independent of CSHR activity (Figure S5 and Table S2, Supporting Information). We therefore conclude that the ionic character of the heme group is important for selective uptake by CSHRs, and that esterification of the propionyl groups increases lipophilicity and contributes toward loss of specificity.

Antimicrobial photodynamic inactivation (aPDI).

Ga-PpIX was initially evaluated as a photosensitizer against a laboratory strain of *S. aureus* (PC 1203). Studies were performed in the context of topical administration using a handheld LED array operating at 405 nm (30 mW/cm^2 per LED), a visible wavelength with no risk of DNA damage. Antimicrobial photodynamic inactivation (aPDI) experiments were performed on bacterial suspensions in 96-well plates; wells were treated with aliquots of Ga-PpIX, followed immediately by a 10-second exposure to 405-nm light using the LED source (140 mW/cm^2; see Experimental Section for complete details). The aPDI activity of Ga-PpIX against *S. aureus* is remarkably rapid and potent, with 10 seconds of irradiation (ca. 1.4 J/cm^2) resulting in a 2.87 ± 0.12 log reduction in colony-forming units (CFU) per mL at 0.03 μM, and complete eradication (> 6 log reduction in CFU/mL) at 0.24 μM (Figure 4a). Light exposure for 30 seconds did not produce a clear increase in potency for aPDI, although eradication was observed at a lower Ga-PpIX dose (Supporting Information). In contrast, Ga-PpIX exhibited only modest bactericidal activity in the absence of light, with a 3-log reduction at approximately 70 μM. The photodynamic effect thus increases the potency of Ga-PpIX against *S. aureus* by over 3 orders of magnitude, relative to its dark toxicity.

The aPDI activity of Ga-PpIX was compared against two other photosensitizers with similar λ_{max} values, under identical conditions: TMPyP (λ_{max} 421 nm), a tetracationic porphyrin that has also been noted for its rapid and potent aPDI,[41,42] and PpIX (λ_{max} 405 nm), the photoactive species generated in situ during clinical aPDT with 5-aminolevulinic acid.[13,14] aPDI studies using the 405-nm LED source show both photosensitizers to be active at this wavelength, but less potent than Ga-PpIX by an order of magnitude (Figure 4a). The dark toxicities of TMPyP and PpIX against this strain were evaluated and determined to be 7.4 μM and 36 μM respectively, meaning that their photodynamic effects increased their potency by less than 2 orders of magnitude.

To establish the efficacy of Ga-PpIX-mediated aPDI against MDR strains of *S. aureus*, we tested several clinical isolates of MRSA known to exhibit resistance to various antibiotics including macrolides, aminoglycosides, lincosamides, and fluoroquinolones (Figure 4b and Table 1). Antimicrobial activity against these strains was achieved using 0.06–0.12 μM Ga-PpIX and 10 seconds of irradiation by the 405-nm LED source; increasing the irradiation time to 30 seconds guaranteed a 3-log reduction in all strains using 0.06 μM, with > 6-log reduction in two cases. These results support our assumption that Ga-PpIX can be developed for aPDT against *S. aureus* infections, regardless of their MDR status. The consistent response to Ga-PpIX treatment is encouraging, as efficacy between strains can vary in antimicrobial photodynamic therapy.[43]

To determine whether Ga-PpIX-mediated aPDI could be achieved using a less powerful light source, experiments were also performed using a 20-W compact fluorescent lightbulb (CFL) with violet light emission near the Soret band of Ga-PpIX (λ_{max} 406 nm; Figure S7, Supporting Information). aPDI against *S. aureus* could be achieved at micromolar concentrations within 5 minutes and <1 μM within 15 minutes exposure to the CFL source, the latter corresponding with a 2-log increase in potency relative to dark toxicity (Figure 5 and Table S3, Supporting Information). Ga-PpIX mediated aPDI against clinical MRSA strains using the CFL source was comparable to that observed with the laboratory *S. aureus* strain (1–5 μM); the aPDI activity of PpIX was also evaluated with CFL irradiation, and found to be less than that of Ga-PpIX as expected (Table S3). Overall, we find that Ga-PpIX can produce respectable levels of aPDI with an off-the-shelf CFL source, when using exposure times on the order of minutes. In this context, it is worth mentioning a recent report in which 5 μM of photosensitizer (TMPyP) was sufficient to produce aPDI using ambient lighting at a power density of 0.13 mW/cm^2, within a 10-minute exposure time.[42]

Cytotoxicity studies.

Ga-PpIX was tested for toxicity against human kidney cells (HEK293) and keratinocytes (HaCaT), the former to address potential systemic effects and the latter for topical exposure with and without light irradiation. HEK293 cells were evaluated for dark toxicity using the MTT assay following a 72-hour incubation with Ga-PpIX from 0.6 μM up to 20 μM, above the limits needed for aPDI based on the response curves in Figure 5. Signs of mitochondrial cytotoxicity were observed starting at 5 μM ($p < 0.05$), however cell viabilities remained above 90% even at the highest concentration (Figure 6a).

Viability assays were also performed with HaCaT cells using 20 μM Ga-PpIX and 10 seconds of irradiation by the LED source, with different incubation times (Figure 6b). Modest dark toxicity was observed after a 22-h incubation period (85% viability; $p > 0.1$), but a 10-s exposure to 405-nm irradiation stimulated cell growth or activity, with no adverse effect by Ga-PpIX (165–170% viability; $p < 0.005$). The stimulation of cell activities by short periods of laser or LED irradiation has been noted by others, particularly in the context of low-level light therapy.[44] We thus conclude that Ga-PpIX mediated aPDI is compatible with mammalian systems, under the conditions presented in this study.

Rapid uptake of Ga-PpIX by other bacterial pathogens.

S. aureus is not the only bacterial species that can express CSHRs enabling rapid hemin acquisition; indeed, studies aimed at elucidating the roles of specific heme transporters in aPDT are just now emerging.[45] To determine whether Ga-PpIX might be considered for targeted aPDT against additional pathogens, we developed a fluorescence imaging assay and screened a diverse panel of Gram-positive and negative bacteria for rapid Ga-PpIX uptake. Based on prior studies,[37] we expected bacteria to fall into three types: (1) those capable of rapid hemin acquisition via expression of CSHRs; (2) those that acquire hemin by the release and recovery of harvesting proteins (hemophores),[46] with a consequent delay in hemin acquisition rate; and (3) species that do not produce hemin-harvesting systems for iron acquisition (Figure 7).

Bacteria were typically cultivated under iron-deficient conditions and treated with Ga-PpIX at a fixed concentration for 15 to 60 minutes, then centrifuged and redispersed in PBS and imaged by fluorescence microscopy using a standard microscope. Those that achieved fluorescence saturation within the first 15 minutes were assigned as Type 1; those that accumulated fluorescence more slowly were assigned as Type 2 (Figure 8 and Table 2). Type 1 bacteria include Gram-positive species such as staphylococci (*S. aureus* and *S. epidermidis*), *Bacillus anthracis*, *Cornyebacterium diphtheria*, and *Streptococcus pneumoniae*. CSHRs for the first four species are well characterized, but the hemin acquisition system for *S. pneumoniae* is currently unassigned and awaits further study.[49,50] We note that at least two Type 1 pathogens are on government watchlists: *B. anthracis* can be weaponized for biological warfare with up to 90% mortality rate upon inhalation or ingestion,[47] and *S, pneumoniae* is a vector for community-acquired pneumonia, especially among young children.[2,3]

To further illustrate the differences in Ga-PpIX uptake between Type 1 and Type 2 bacteria, we performed confocal fluorescence microscopy on *S. aureus* and *Yersinia enterocolitica*, a Gram-negative species that acquires hemin through HemR, a TonB-dependent hemophore receptor.[48] As expected, *S. aureus* was strongly and uniformly labelled within the first 15 minutes, indicative of saturation; in contrast, the fluorescence of *Y. enterocolitica* was initially weak and heterogeneous but gradually increased over a 60-minute period (Figure 9). This supports our hypothesis that hemin (or Ga-PpIX) acquisition by Type 2 bacteria is delayed by the extra step of hemophore retrieval (Figure 7).

In conclusion, CSHR-expressing pathogens such as *S. aureus* can be targeted for potent photodynamic inactivation within seconds using Ga-PpIX and 405-nm light irradiation. A structure–activity study reveals the importance of ionic character and the presence of free propionyl units in the specific uptake of Ga-PpIX. Antimicrobial activity is achieved with nanomolar Ga-PpIX using a monochromatic LED source; a lower but still respectable level of aPDI could be achieved with micromolar Ga-PpIX using an off-the-shelf CFL source. Ga-PpIX is highly active against several strains of MRSA, yet exhibits low dark toxicity against HEK293 cells and negligible phototoxicity against HaCaT cells under aPDI conditions, paving the path toward *in vivo* studies using skin infection models. Lastly, rapid Ga-PpIX uptake by several other (Type 1) pathogens has been established, broadening its potential scope for targeted aPDT.

Experimental Section

Hemin chloride and all reagents were obtained from commercial sources, and used as received unless otherwise noted (see Supporting Information). The optimized synthesis of Ga-PpIX (**1**),[49] PpIX (**2**),[50] and derivatives **6**, **11**, and **12** are described in Supporting Information; the synthesis of Zn-PpIX (**3**),[51] hematoporphyrin (HP; **4**) and Zn-HP (**5**),[52] PpIX dimethyl diester (**7**)[53], HP dimethyl diester (**8**)[61], and di-*O*-acetyl- and di-*O*-succinyl-HP dimethyl diester (**9**, **10**)[54] were synthesized from PpIX or HP as previously described in the literature. Absorption spectra were collected on a Varian Cary50 spectrometer. Photoemissions were measured on a Cary Eclipse fluorimeter with a gate time of 5 ms. EPR spectra were obtained using a Bruker EMX X-band spectrometer operating at 9.5 GHz and 5.02 mW, with a field modulation amplitude of 5 *g* at 100 kHz. Flow cytometry was performed using a BD Accuri C6 instrument ($\lambda_{ex}/\lambda_{em}$ = 488/585 nm). Fluorescence images were acquired using an upright microscope with Hg lamp and filter set for λ_{em} > 570 nm (Olympus BX51, U-MWG2), or a laser scanning confocal microscope with 488-nm excitation and appropriate bandpass filter (Olympus FV1000, DM405/488; BA505–605). Care was taken to minimize UV or laser exposure time to less than 5 seconds to avoid bleaching of molecules. Fluorescence data analyses were performed in triplicate using Image J 1.47v, based on mean pixel intensities from labelled bacteria (8-bit format).

Microbiological culture conditions.

Bacterial strains were obtained from the American Type Culture Collection (ATCC), BEI Resources, or Microbiologics, and cultured at 37 °C in an aerobic atmosphere unless otherwise noted. Bacterial suspensions were typically incubated for up to 16 hours until an optical density of 1.0 was achieved at 600 nm. Bacterial counts were estimated in units of CFU/mL by plating serial dilutions onto agar plates, followed by incubation for 16 hours at 37 °C. Iron-challenged conditions were typically achieved by first growing the bacteria in standard (iron-replete) media, then in media containing 3 mM 2,2'-bipyridine (Table 2). Further details and variations on bacterial culture conditions are provided in Supporting Information.

Bacterial uptake assays of Ga-PpIX and related derivatives.

Bacteria were cultured and assayed in iron-deficient media unless otherwise noted. A stock solution of Ga-PpIX (200 μM) was prepared by dispersing 2.54 mg in 1 mL of 10% DMSO in PBS for 10 minutes protected from light, followed by filtration and 20-fold dilution in PBS just prior to use. For flow cytometry, bacterial suspensions (10^8 CFU in 0.5 mL) were incubated with Ga-PpIX (73 μM) for specified periods (10 s–40 min), then fixed with 0.5 mL of 4% paraformaldehyde and subjected to analysis without further processing. A region of interest (ROI) based on forward scatter (FSC) and side scatter (SSC) parameters was used to gate bacterial populations (ca. 5×10^4 per data point) to exclude fluorescent debris.[55] For fluorescence imaging, bacterial suspensions (10^8 CFU in 0.5 mL) were incubated with Ga-PpIX or related derivatives (73 μM) for 15 min, then centrifuged and resuspended twice in 0.5 mL deionized water, then deposited onto glass slides in 10-μL aliquots and dried in air. More details on image processing and flow cytometry analysis are provided in Supporting Information (Figures S3–S5).

Competitive hemin uptake assay.

Suspensions of *S. aureus* (PCI 1203) were centrifuged and redispersed 3 × in 0.5 mL PBS, and adjusted to a concentration of 10^8 CFU/mL. Stock solutions of hemin and PpIX derivatives **1–13** were mixed in a 1:1 ratio (0.5 mL), then added to bacterial suspensions (10^8 CFU in 0.5 mL) and incubated for 15 min at room temperature. For control studies, hemin or fluorophore solutions were substituted with PBS to maintain constant concentration. Bacteria were harvested and washed as described above, then evaluated by fluorescence microscopy for relative uptake efficiency.

Antimicrobial photodynamic inactivation (aPDI).

Studies were performed in triplicate using 96-well microtiter plates with irradiation from a 405-nm LED array (Rainbow Technology Systems, 140 mW/cm^2) or a 20-W compact fluorescent lightbulb (CFL; Sunlite SL20/BLB) housed in an ellipsoidal reflector dome with emission at 406 nm (*ca.* 12.4 mW/cm^2; see Supporting Information). Antimicrobial assays were performed on planktonic bacteria at 10^7 CFU/mL with variable exposure times to CFL irradiation, followed by plating on agar and incubation at 37 °C. In a typical experiment, bacterial suspensions were transferred into microtiter plates then treated with 100-μL aliquots of Ga-PpIX with final concentrations ranging from 0.03 to 120 μM, followed immediately with LED irradiation (10 seconds) or CFL irradiation (up to 15 minutes). The irradiated bacteria were plated onto agar in serial tenfold dilutions (10^7–10^1 CFU/mL); controls included one set of wells without photosensitizer (Ctrl$^+$) and one set of wells with photosensitizer but without irradiation (dark toxicity). Bacterial counts were determined by the drop-plate method using TS–agar plates,[56] and recorded as mean log values with an error of one standard deviation. Bacterial susceptibilities were quantified by subtracting mean log values from an initial value of 7, with the threshold for antimicrobial activity defined as a 3-log reduction in cell count.

Cytotoxicity (MTT oxidation) assays.

HEK293 cells (ATCC CRL-1573) and HaCaT cells (AddexBio) were cultured in DMEM containing 10% FBS, and incubated at 37 °C in a 5% CO_2 atmosphere, with multiple passages before use. Trypsinized cells were added to 96-well microtiter plates (10^4 cells/well) and incubated for 18–24 hours before treatment with Ga-PpIX (100 μM stock solution), with final concentrations ranging from 0.6 to 20 μM. Control wells were treated with DMEM/FBS (Ctrl$^+$) or 0.005% Triton X-100 in media (Ctrl$^-$). HEK293 cells were incubated for 72 hours, then treated with MTT (5 mg/mL, 10 μL/well) and incubated for another 4 hours at 37 °C. HaCaT cells were treated with 20 μM Ga-PpIX and irradiated for 10 seconds using the 405-nm LED source, then incubated for 0 or 22 hours prior to MTT treatment. All cells were fixed by adding 0.1 M HCl in isopropanol containing 10% Triton X-100 (100 μL/well) and mixed for 12 hours on a plate rocker in dark at room temperature. Absorbance readings were acquired at 570 nm (main absorbance) and 650 nm (background).

Supplementary Material

Refer to Web version on PubMed Central for supplementary material.

Acknowledgments.

The authors acknowledge financial support from the Department of Defense (W911SR-08-C-0001) through the U.S. Army RDECOM (Edgewood Contracting Division), the National Science Foundation (CMMI-1449358), the National Institutes of Health (R01 AI130186), and the Purdue University Center for Cancer Research (P30 CA023168). We thank BEI Resources at NIAID for providing several of the bacterial strains used in this study, David McMillin for assistance with fluorimetry, María Mercado Ojeda and Zackery Hernandez for contributions toward antimicrobial studies, Gregory Knipp for providing HEK293 cells, and Kathy Raghed and J. Paul Robinson for their kind assistance with flow cytometry.

References

1. Tarai B, Das P, and Kumar D (2013) Recurrent challenges for clinicians: Emergence of methicillin-resistant Staphylococcus aureus, vancomycin resistance, and current treatment options. J. Lab. Physicians 5, 71–78. DOI: 10.4103/0974-2727.119843. [PubMed: 24701097]
2. Antibiotic Resistance Threats in the United States. (2013) Centers for Disease Control and Prevention: Atlanta.
3. World Health Organization (2014). Antimicrobial resistance: Global report on surveillance. Fact Sheet No. 194
4. Rodvold KA and McConeghy KW (2014) Methicillin-Resistant Staphylococcus aureus Therapy: Past, Present, and Future. Clin. Infect. Dis 58, S20–S27. DOI: 10.1093/cid/cit614. [PubMed: 24343828]
5. Gu B; Kelesidis T, Tsiodras S, Hindler J, and Humphries RM (2013) The emerging problem of linezolid-resistant Staphylococcus. J. Antimicrob. Chemother 68, 4–11. DOI: 10.1093/jac/dks354. [PubMed: 22949625]
6. Skiest DJ (2006) Treatment Failure Resulting from Resistance of Staphylococcus aureus to Daptomycin. J. Clin. Microbiol 44, 655–656. DOI: 10.1128/jcm.44.2.655-656.2006. [PubMed: 16455939]
7. Chambers HF and DeLeo FR (2009) Waves of Resistance: Staphylococcus aureus in the Antibiotic Era. Nat. Rev. Microbiol 7, 629–641. DOI: 10.1038/nrmicro2200. [PubMed: 19680247]
8. Wainwright M (1998) Photodynamic antimicrobial chemotherapy (PACT). J. Antimicrob. Chemother 42, 13–28. DOI: 10.1093/jac/42.1.13. [PubMed: 9700525]
9. Hamblin MR; Hasan T (2004) Photodynamic therapy: A new antimicrobial approach to infectious disease? Photochem. Photobiol. Sci 3, 436–450. DOI: 10.1039/b311900a. [PubMed: 15122361]
10. Giuliani F, Martinelli M, Cocchi A, Arbia D, Fantetti L, and Roncucci G (2010) In vitro resistance selection studies of RLP068/Cl, a new Zn(II) phthalocyanine suitable for antimicrobial photodynamic therapy. Antimicrob. Agents Chemother 54, 637–642. DOI: 10.1128/aac.00603-09. [PubMed: 20008782]
11. Agrawal T, Avci P, Gupta GK, Rineh A, Lakshmanan S, Batwala V, Tegos GP, and Hamblin MR (2015) Harnessing the power of light to treat staphylococcal infections focusing on MRSA. Curr. Pharm. Des 21, 2109–2121. DOI: 10.2174/1381612821666150310102318. [PubMed: 25760339]
12. Zeina B, Greenman J, Corry D, and Purcell WM (2003) Antimicrobial photodynamic therapy: Assessment of genotoxic effects on keratinocytes in vitro. Br. J. Dermatol 148, 229–232. [PubMed: 12588372]
13. Hongcharu W, Taylor CR, Aghassi D, Suthamjariya K, Anderson RR, and Chang Y (2000) Topical ALA-Photodynamic Therapy for the Treatment of Acne vulgaris. J. Invest. Dermatol 115, 183–192. DOI: 10.1046/j.1523-1747.2000.00046.x [PubMed: 10951234]
14. Itoh Y, Ninomiya Y, Tajima S, and Ishibashi A (2000) Photodynamic therapy for Acne vulgaris with topical 5-aminolevulinic acid. Arch. Dermatol 136, 1093–1095. DOI: 10.1001/archderm.136.9.1093. [PubMed: 10987863]
15. Andreas B, Claudia D, Felix K, and Søren J (2008) Short-term clinical effects of adjunctive antimicrobial photodynamic therapy in periodontal treatment: A randomized clinical trial. J. Clin. Periodontol 35, 877–884. DOI: 10.1111/j.1600-051X.2008.01303.x [PubMed: 18713259]

16. Sigusch BW, Engelbrecht M, Völpel A, Holletschke A, Pfister W, and Schütze J (2010) Full-Mouth Antimicrobial Photodynamic Therapy in Fusobacterium nucleatum–Infected Periodontitis Patients. J. Periodontol 81, 975–981. DOI: 10.1902/jop.2010.090246. [PubMed: 20350153]

17. Cassidy CM, Tunney MM, McCarron PA, and Donnelly RF (2009) Drug delivery strategies for photodynamic antimicrobial chemotherapy: From benchtop to clinical practice. J. Photochem. Photobiol. B 95, 71–80. DOI: 10.1016/j.jphotobiol.2009.01.005. [PubMed: 19223196]

18. Kharkwal GB, Sharma SK, Huang Y-Y, Dai T, and Hamblin MR (2011) Photodynamic Therapy for Infections: Clinical Applications. Lasers Surg. Med 43, 755–767. DOI: 10.1002/lsm.21080. [PubMed: 22057503]

19. Maisch T, Hackbarth S, Regensburger J, Felgenträger A, Bäumler W, Landthaler M, and Röder B (2011) Photodynamic inactivation of multi-resistant bacteria (PIB) – a new approach to treat superficial infections in the 21st century. J. Dtsch. Dermatol. Ges 9, 360–366. DOI: 10.1111/j.1610-0387.2010.07577.x [PubMed: 21114627]

20. Septimus EJ and Schweizer ML (2016) Decolonization in Prevention of Health Care-Associated Infections. Clin. Microbiol. Rev 29, 201–222. DOI: 10.1128/CMR.00049-15. [PubMed: 26817630]

21. Alonso C and Boyle RW (2010) Bioconjugates of Porphyrins and Related Molecules for Photodynamic Therapy. In Handbook of Porphyrin Science, Kadish KM; Smith KM; Guilard R, Eds. World Scientific: Vol. 4, pp 121–190. DOI: 10.1142/9789814280228_0017.

22. Dickson EFG, Kennedy JC, Pottier RH, and Patrice T (2003) Photodynamic therapy using 5-aminolevulinic acid-induced protoporphyrin IX. In Photodynamic Therapy, Patrice T, Ed., Royal Society of Chemistry: Cambridge, pp. 81–104. DOI: 10.1039/9781847551658-00081.

23. Malik Z, Hanania J, and Nitzan Y (1990) New trends in photobiology bactericidal effects of photoactivated porphyrins-- An alternative approach to antimicrobial drugs, J. Photochem. Photobiol. B 5, 281–293. DOI: 10.1016/1011-1344(90)85044-W. [PubMed: 2115912]

24. Pilpa RM, Robson SA, Villareal VA, Wong ML, Phillips M, and Clubb RT (2009) Functionally distinct NEAT (NEAr Transporter) domains within the Staphylococcus aureus IsdH/HarA protein extract heme from methemoglobin, J. Biol. Chem 284, 1166–1176. DOI: 10.1074/jbc.M806007200. [PubMed: 18984582]

25. Azad BB, Cho CF, Lewis JD, and Luyt LG (2012) Synthesis, radiometal labelling and in vitro evaluation of a targeted PPIX derivative, Appl. Radiat. Isotop 70, 505–511. DOI: 10.1016/j.apradiso.2011.11.054.

26. Hu Y, Geissinger P, and Woehl JC (2011) Potential of protoporphyrin IX and metal derivatives for single molecule fluorescence studies. J. Luminescence 131, 477–481. DOI: 10.1016/j.jlumin.2010.12.012

27. Bonnett R and Martínez G (2001) Photobleaching of sensitisers used in photodynamic therapy. Tetrahedron 57, 9513–9547. DOI: 10.1016/S0040-4020(01)00952-8.

28. Stojiljkovic I, Kumar V, and Srinivasan N (1999) Non-iron metalloporphyrins: Potent antibacterial compounds that exploit haem/Hb uptake systems of pathogenic bacteria. Mol. Microbiol 31, 429–442. DOI: 10.1046/j.1365-2958.1999.01175.x. [PubMed: 10027961]

29. Wilks A and Barker KD (2010) Mechanisms of Heme Uptake and Utilization in Bacterial Pathogens, In Handbook of Porphyrin Science (Kadish KM, Smith KM, and Guilard R, Eds.), pp 357–398, World Scientific, Singapore DOI:10.1142/9789814322386_0024.

30. Olczak T, Maszczak-Seneczko D, Smalley JW, and Olczak M (2012) Gallium(III), cobalt(III) and copper(II) protoporphyrin IX exhibit antimicrobial activity against Porphyromonas gingivalis by reducing planktonic and biofilm growth and invasion of host epithelial cells, Arch. Microbiol 194, 719–724. DOI: 10.1007/s00203-012-0804-3. [PubMed: 22447101]

31. Arivett BA, Fiester SE, Ohneck EJ, Penwell WF, Kaufman CM, Relich RF, and Actis LA (2015) Antimicrobial Activity of Gallium Protoporphyrin IX against Acinetobacter baumannii Strains Displaying Different Antibiotic Resistance Phenotypes. Antimicrob. Agents Chemother 59, 7657–7665. DOI: 10.1128/aac.01472-15 [PubMed: 26416873]

32. Bhaumik J (2007) Synthetic Porphyrinic Macrocycles for Photodynamic Therapy and Other Biological Applications, Ph.D. Thesis, North Carolina State University, Raleigh, NC.

33. Hammer ND and Skaar EP (2011) Molecular mechanisms of Staphylococcus aureus iron acquisition. Annu. Rev. Microbiol 65, 129–147. DOI: 10.1146/annurev-micro-090110-102851. [PubMed: 21639791]
34. Maresso AW, Garufi G, and Schneewind O (2008) Bacillus anthracis secretes proteins that mediate heme acquisition from hemoglobin. PLoS. Pathog 4, e1000132 DOI: 10.1371/journal.ppat.1000132. [PubMed: 18725935]
35. Nakamura K, Ishiyama K, Ikai H, Kanno T, Sasaki K, Niwano Y, and Kohno M (2011) Reevaluation of analytical methods for photogenerated singlet oxygen. J. Clin. Biochem. Nutr 49, 87–95. DOI: 10.3164/jcbn.10-125. [PubMed: 21980223]
36. Frederiksen PK, McIlroy SP, Nielsen CB, Nikolajsen L, Skovsen E, Jørgensen M, Mikkelsen KV, and Ogilby PR (2005) Two-Photon Photosensitized Production of Singlet Oxygen in Water. J. Am. Chem. Soc 127, 255–269. DOI: 10.1021/ja0452020. [PubMed: 15631475]
37. Maltais TR, Adak AK, Younis W, Seleem MN, and Wei A (2016) Label-free detection and discrimination of bacterial pathogens based on hemin recognition. Bioconjugate Chem. 27, 1713–1722. DOI: 10.1021/acs.bioconjchem.6b00236.
38. Carpenter BM, Whitmire JM, and Merrell DS (2009) This is not your mother's repressor: The complex role of fur in pathogenesis. Infect. Immun 77, 2590–2601. DOI: 10.1128/iai.00116-09. [PubMed: 19364842]
39. Wakeman CA, Stauff DL, Zhang Y, and Skaar EP (2014) Differential Activation of Staphylococcus aureus Heme Detoxification Machinery by Heme Analogues. J. Bacteriol 196, 1335–1342. DOI: 10.1128/jb.01067-13. [PubMed: 24443529]
40. Moriwaki Y, Caaveiro JMM, Tanaka Y, Tsutsumi H, Hamachi I, and Tsumoto K (2011) Molecular basis of recognition of antibacterial porphyrins by heme-transporter IsdH-NEAT3 of Staphylococcus aureus. Biochemistry 50, 7311–7230. DOI: 10.1021/bi200493h. [PubMed: 21797259]
41. Eichner A, Gonzales FP, Felgentrager A, Regensburger J, Holzmann T, Schneider-Brachert W, Baumler W, and Maisch T (2013) Dirty hands: photodynamic killing of human pathogens like EHEC, MRSA and Candida within seconds, Photochem. Photobiol. Sci 12, 135–147. DOI: 10.1039/C2PP25164G. [PubMed: 22855122]
42. Eckl DB, Dengler L, Nemmert M, Eichner A, Bäumler W, and Huber H (2018) A Closer Look at Dark Toxicity of the Photosensitizer TMPyP in Bacteria, Photochem. Photobiol 94, 165–172. DOI: 10.1111/php.12846. [PubMed: 28940456]
43. Nakonieczna J and Grinholc M (2012) Photodynamic inactivation requires innovative approach concerning numerous bacterial isolates and multicomponent sensitizing agents, Photodiagn. Photodyn. Ther 9, 359–361. DOI: 10.1016/j.pdpdt.2012.04.002.
44. Hashmi J, Huang Y, Sharma S, Kurup D, De Taboada L, Carroll J, and Hamblin M (2010) Effect of pulsing in low-level light therapy. Lasers Surg. Med 42, 450–466. DOI: 10.1002/lsm.20950. [PubMed: 20662021]
45. Nakonieczna J, Kossakowska-Zwierucho M, Filipiak M, Hewelt-Belka W, Grinholc M, and Bielawski K (2015) Photoinactivation of Staphylococcus aureus using protoporphyrin IX: the role of haem-regulated transporter HrtA, Appl. Microbiol. Biotechnol 100, 1393–1405. DOI: 10.1007/s00253-015-7145-5. [PubMed: 26631186]
46. Crosa JH, Mey AR, and Payne SM (2004) Iron Transport in Bacteria; ASM Press: Washington, D.C. DOI:10.1128/9781555816544.
47. Spencer RC Bacillus anthracis. (2003) J. Clin. Pathol 56, 182–187. DOI: 10.1136/jcp.56.3.182. [PubMed: 12610093]
48. Stojiljkovic I and Hantke K (1992) Hemin uptake system of Yersinia enterocolitica: similarities with other TonB-dependent systems in Gram-negative bacteria. EMBO J. 11, 4359–4367. DOI: 10.1093/emboj/11.12.4359. [PubMed: 1425573]
49. Bohle DS, Dodd EL, Pinter TBJ, and Stillman M (2012) Soluble diamagnetic model for malaria pigment: Coordination chemistry of gallium(III)protoporphyrin-IX. Inorg. Chem 51, 10747–10761. DOI: 10.1021/ic301106g. [PubMed: 23030718]
50. Erdman JG, Ramsey VG, Kalenda NW, and Hanson WE (1956) Synthesis and properties of porphyrin vanadium complexes. J. Am. Chem. Soc 78, 5844–5847. DOI: 10.1021/ja01603a037.

51. Clark E and Kurtz DM (2017) Photosensitized H_2 production using a zinc porphyrin-substituted protein, platinum nanoparticles, and ascorbate with no electron relay: participation of Good's buffers. Inorg. Chem 56, 4584 DOI: 10.1021/acs.inorgchem.7b00228.
52. Xu S, Hu B, Cui Q, Zhou W, Luo H, and Liu Z (2011) Synthesis of 3,8-bisacetyl deuteroporphyrin dimethyl ester. Chin. J. Appl. Chem 28, 657–661. DOI: 10.3724/sp.j.1095.2011.00459.
53. Byrne CJ and Ward AD (1988) A facile porphyrin esterification/etherification procedure. Tetrahedron Lett. 1988, 29, 1421–1424. DOI: 10.1016/S0040-4039(00)80313-5.
54. Bonnett R, Buckley DG, and Hamzetash D (1981) On the nature of 'haematoporphyrin derivative'. J. Chem. Soc., Perkin Trans 1, 3135–3140. DOI: 10.1039/P19810003135.
55. Benincasa M, Barrière Q, Runti G, Pierre O, Bourge M, Scocchi M, and Mergaert P (2016) Single Cell Flow Cytometry Assay for Peptide Uptake by Bacteria. Bio-Protocol 6, e2038 DOI: 10.21769/BioProtoc.2038.
56. Herigstad B, Hamilton M, and Heersink J (2001) How to optimize the drop plate method for enumerating bacteria, J. Microbiol. Methods 44, 121–129. DOI: 10.1016/S0167-7012(00)00241-4. [PubMed: 11165341]
57. Allen CE and Schmitt MP (2009) HtaA is an iron-regulated hemin binding protein involved in the utilization of heme iron in Corynebacterium diphtheriae. J. Bacteriol 191, 2638–2648. DOI: 10.1128/jb.01784-08. [PubMed: 19201805]
58. Tai SS, Lee CJ, and Winter RE (1993) Hemin utilization is related to virulence of Streptococcus pneumoniae. Infect. Immun 61, 5401–5405. DOI: n/a [PubMed: 8225615]
59. Romero-Espejel ME, Gonzalez-Lopez MA, and de Jesus Olivares-Trejo J (2013) Streptococcus pneumoniae requires iron for its viability and expresses two membrane proteins that bind haemoglobin and haem, Metallomics 5, 384–389. DOI: 10.1039/c3mt20244e. [PubMed: 23487307]
60. McConnell MJ, Actis L, and Pachon J (2013) Acinetobacter baumannii: human infections, factors contributing to pathogenesis and animal models, FEM Microbiol. Rev 37, 130–155. DOI: 10.1111/j.1574-6976.2012.00344.x.
61. Zimbler D, Penwell W, Gaddy J, Menke S, Tomaras A, Connerly P, and Actis L (2009) Iron acquisition functions expressed by the human pathogen Acinetobacter baumannii, BioMetals 22, 23–32. DOI: 10.1007/s10534-008-9202-3. [PubMed: 19130255]
62. Eijkelkamp BA, Hassan KA, Paulsen IT, and Brown MH (2011) Investigation of the human pathogen Acinetobacter baumannii under iron limiting conditions, BMC Genomics 12, 126 DOI: 10.1186/1471-2164-12-126. [PubMed: 21342532]
63. Torres AG and Payne SM (1997) Haem iron-transport system in enterohaemorrhagic Escherichia coli O157:H7, Mol. Microbiol 23, 825–833. DOI: 10.1046/j.1365-2958.1997.2641628.x. [PubMed: 9157252]
64. Fouts DE, Tyler HL, DeBoy RT, Daugherty S, Ren Q, Badger JH, Durkin AS, Huot H, Shrivastava S, Kothari S, et al. (2008) Complete Genome Sequence of the N2-Fixing Broad Host Range Endophyte Klebsiella pneumoniae 342 and Virulence Predictions Verified in Mice, PLoS Genetics 4, e1000141 DOI: 10.1371/journal.pgen.1000141. [PubMed: 18654632]

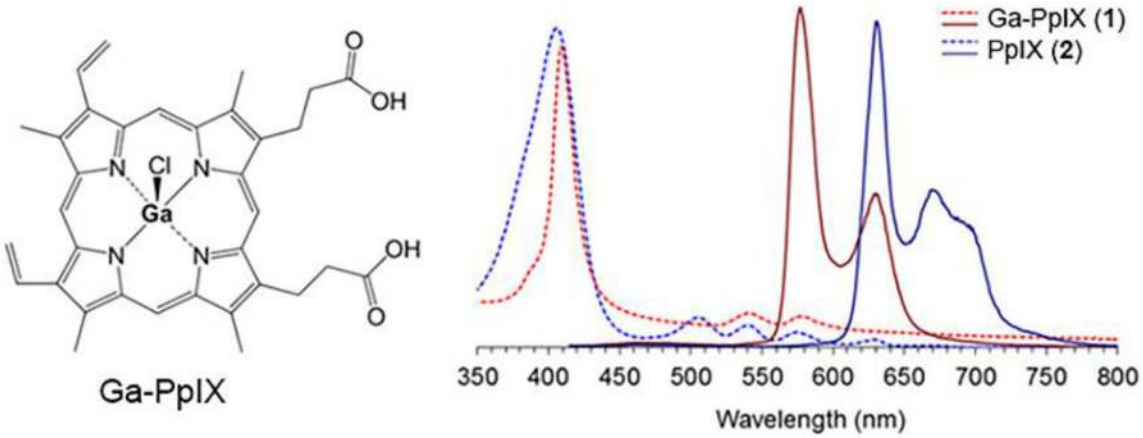

Figure 1.

Absorbance (---) and emission (—) spectra for Ga-PpIX (8 μM in DMSO, red) with comparison to PpIX (blue). Structure of Ga-PpIX shown at left.

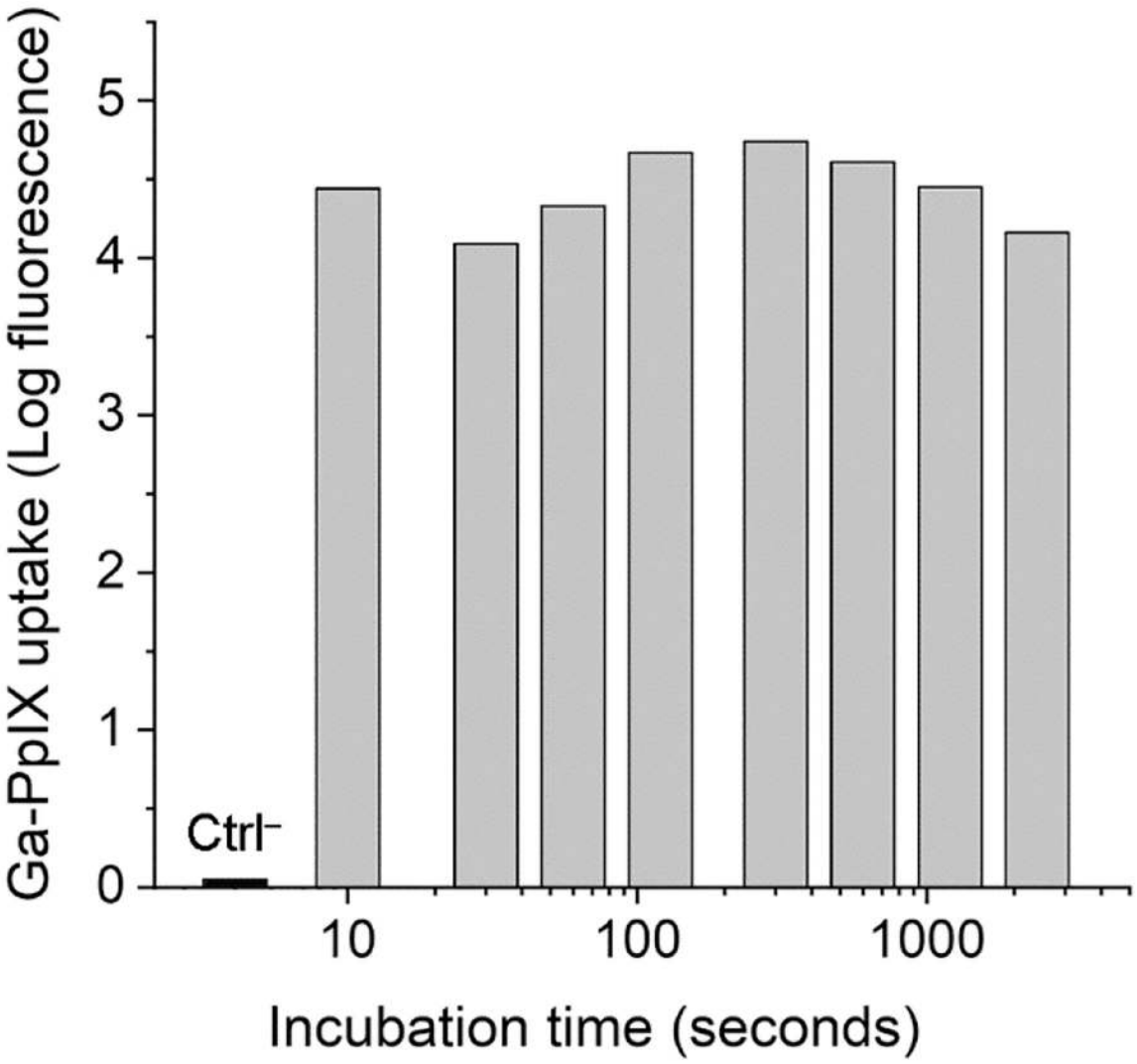

Figure 2.

Flow cytometry of *S. aureus* treated with Ga-PpIX as a function of incubation time (plotted on log scale; $Ctrl^{-}$ = no Ga-PpIX). Bacteria were fixed with paraformaldehyde prior to analysis. All runs based on gated bacteria populations and reported as mean fluorescence values.

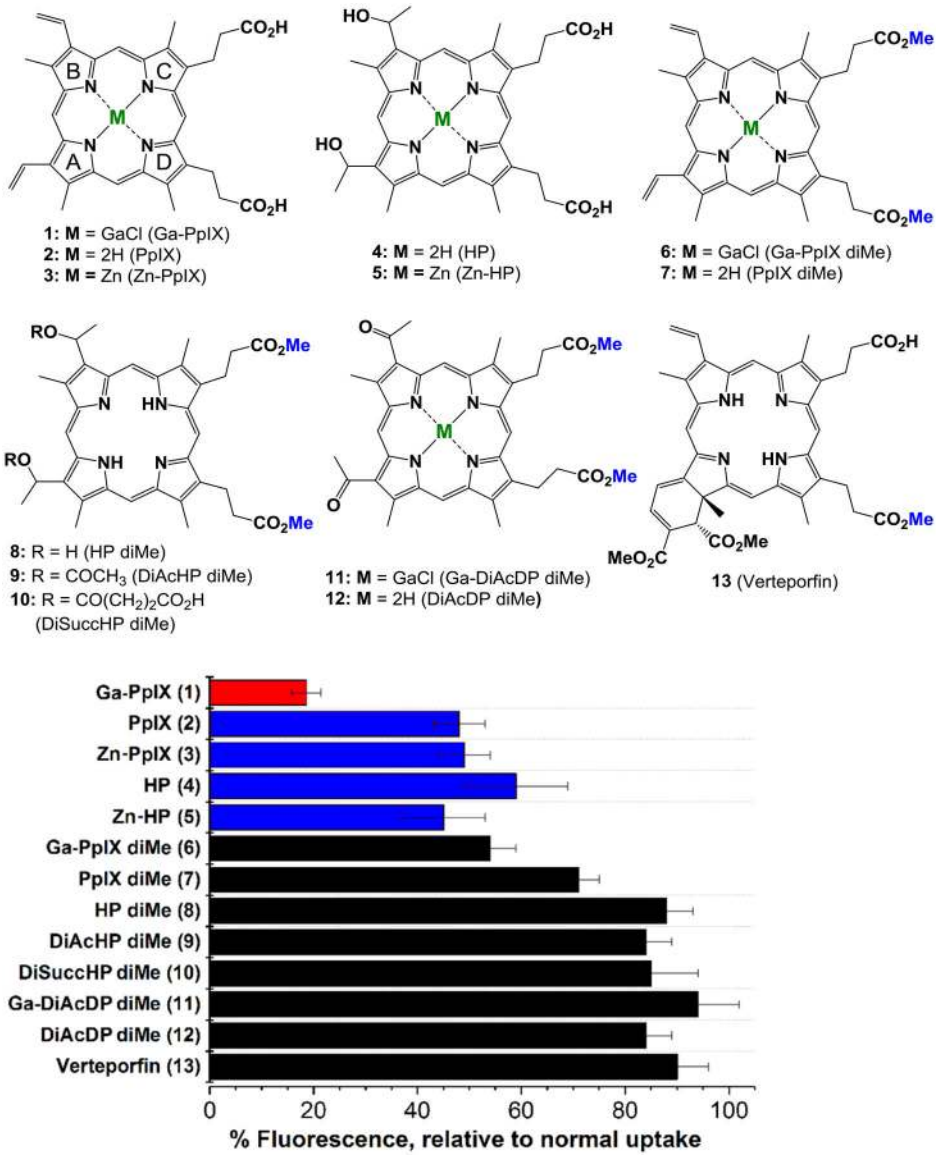

Figure 3.

Competitive uptake of PpIX derivatives **1–13** by *S. aureus* (PCI 1203) versus one equivalent of hemin (15 min co-exposure). Ga-PpIX **1** uptake inhibition (red) is greater than that of other PpIX diacid and diester derivatives (blue and black, respectively). All values are relative to uptake in the absence of hemin; see Supporting Information for complete details.

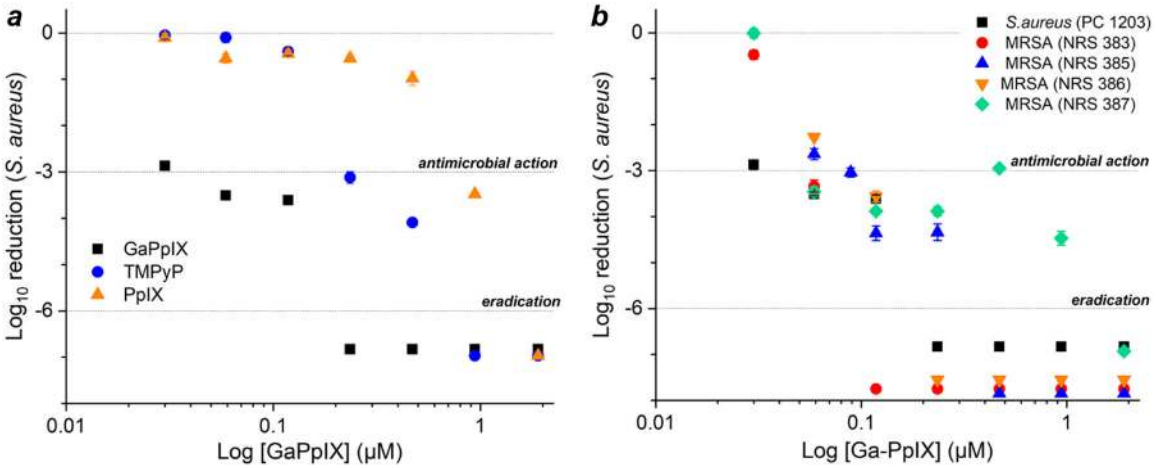

Figure 4.

(a) Antimicrobial photodynamic inactivation of *S. aureus* (PC 1203, ATCC 10537) using Ga-PpIX in PBS (pH 7.4), with 10-second exposure to 405-nm light from a LED array (1.4 J/cm^2). aPDI activities of two other photosensitizers (TMPyP and PpIX) were evaluated under identical conditions for comparison. (b) aPDI activity of Ga-PpIX against several clinical isolates of MRSA. Bacteria were plated after irradiation and incubated at 37 °C for 20 h to obtain log reduction values; antimicrobial action and eradication correspond to 3- and 6-log reductions in CFU/mL, respectively. All experiments were performed in triplicate.

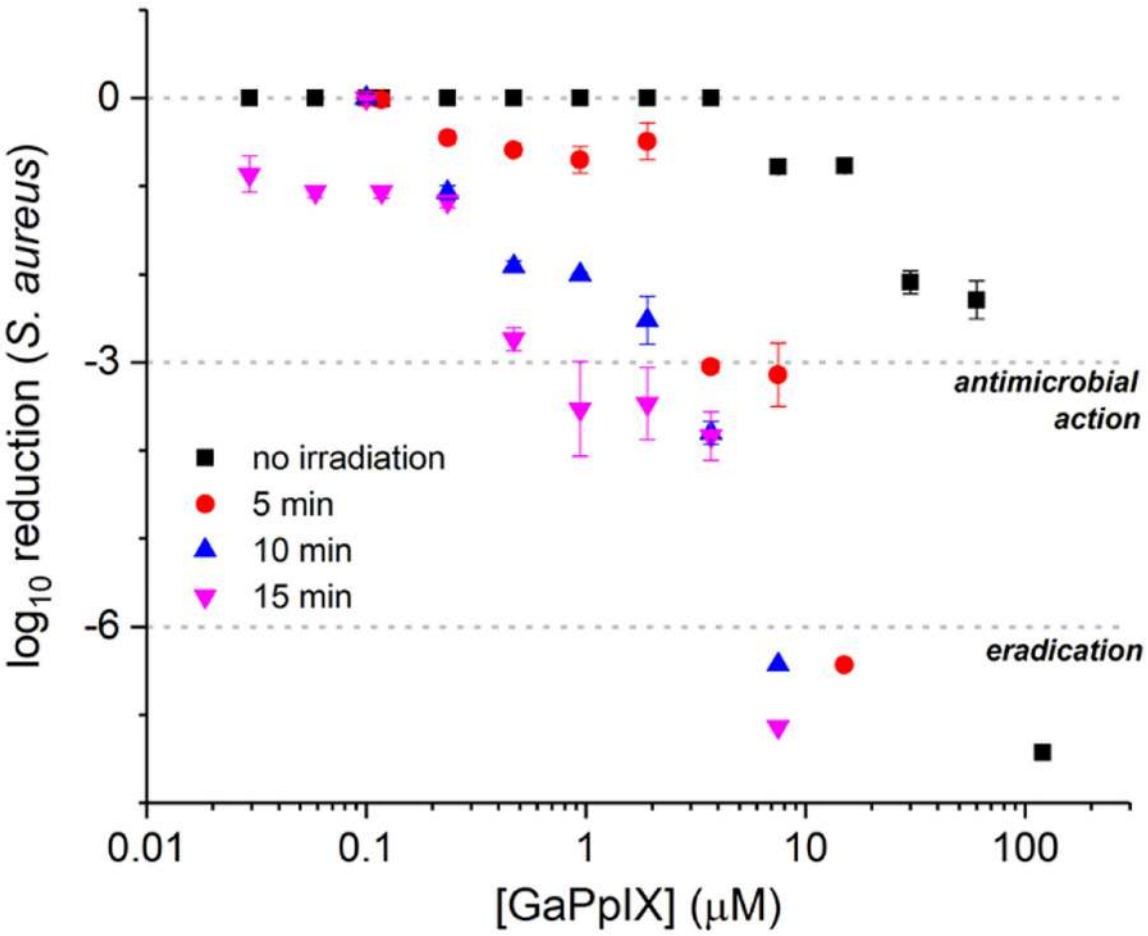

Figure 5.

Normalized survival plots of *S. aureus* (PC 1203) as a function of Ga-PpIX concentration and exposure time to 406-nm light from a 20-W compact fluorescent lightbulb (CFL). Antimicrobial action and eradication correspond to 3- and 6-log CFU/mL reduction, respectively.

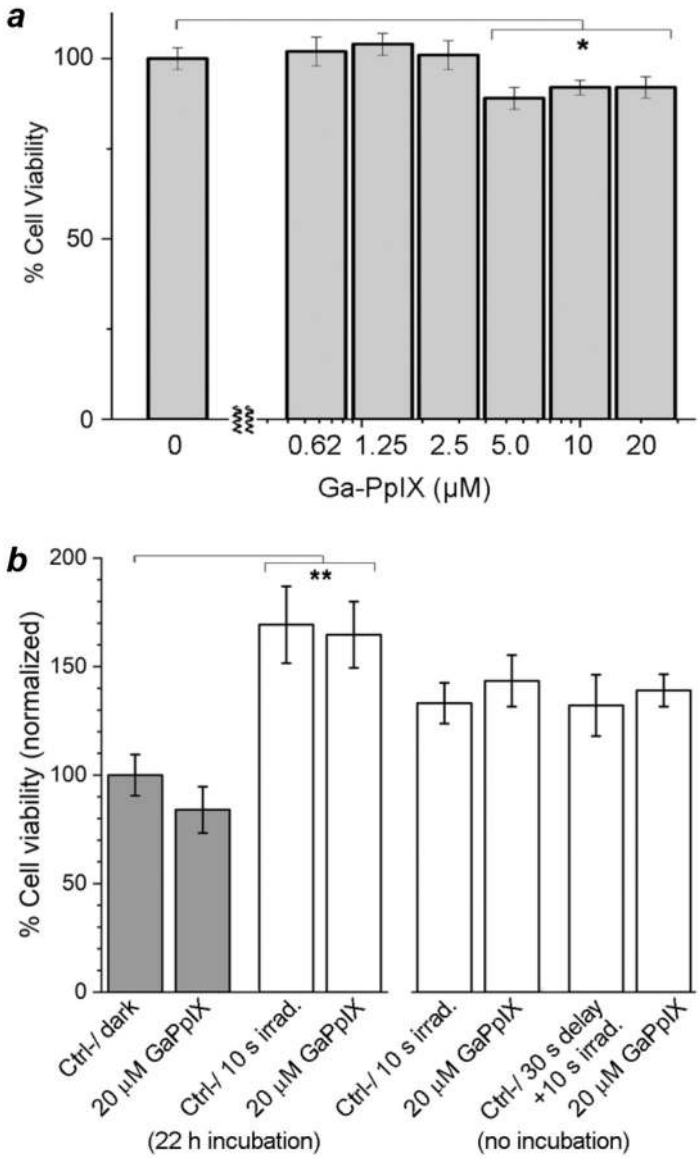

Figure 6.

(a) Cytotoxicity of Ga-PpIX against HEK293 cells versus concentration; * $p < 0.05$ (N=3). (b) Effects of Ga-PpIX (20 μM) and 405-nm irradiation (10-s LED exposure) on HaCaT cells with different incubation times following treatment. Dark controls (no light exposure) presented in dark grey; ** $p < 0.005$ (N=3). A complete set of p values is provided in Supporting Information (Tables S4, S5).

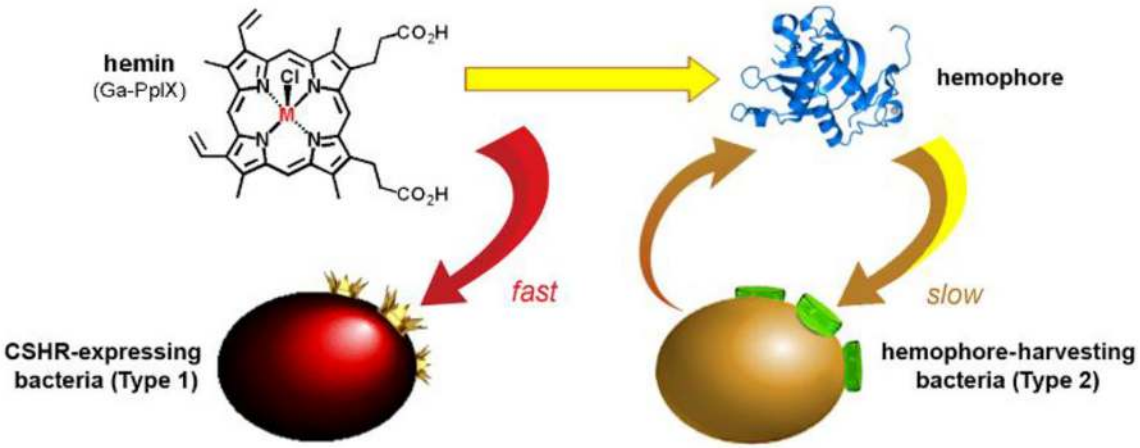

Figure 7.
CSHR-expressing bacteria (Type 1) and hemophore-harvesting strains (Type 2), distinguished by their rates of hemin (or Ga-PpIX) uptake.[37]

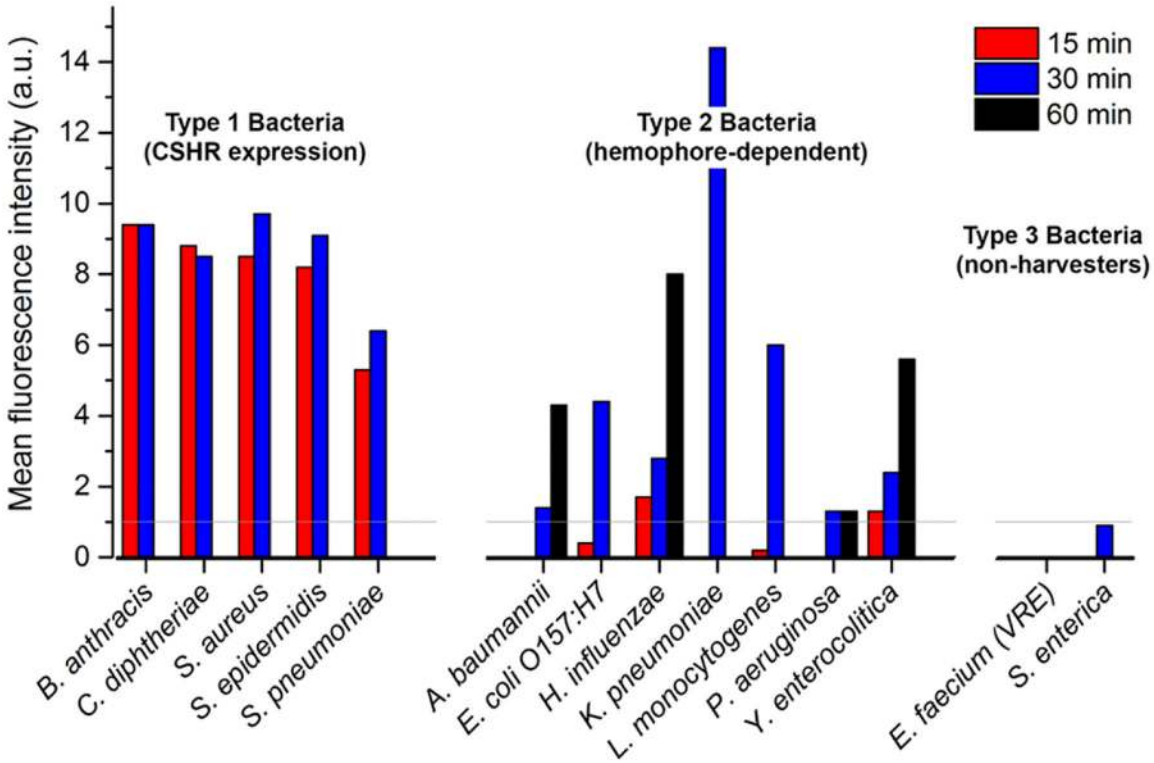

Figure 8.

Ga-PpIX uptake by representative bacteria, classified into three types based on rates of saturation. Threshold of significance (grey line) is defined by the autofluorescence of *S. enterica*, a Type 3 species, and set at a unit value of one. Data for image analysis collected in triplicate; see Supporting Information for complete details.

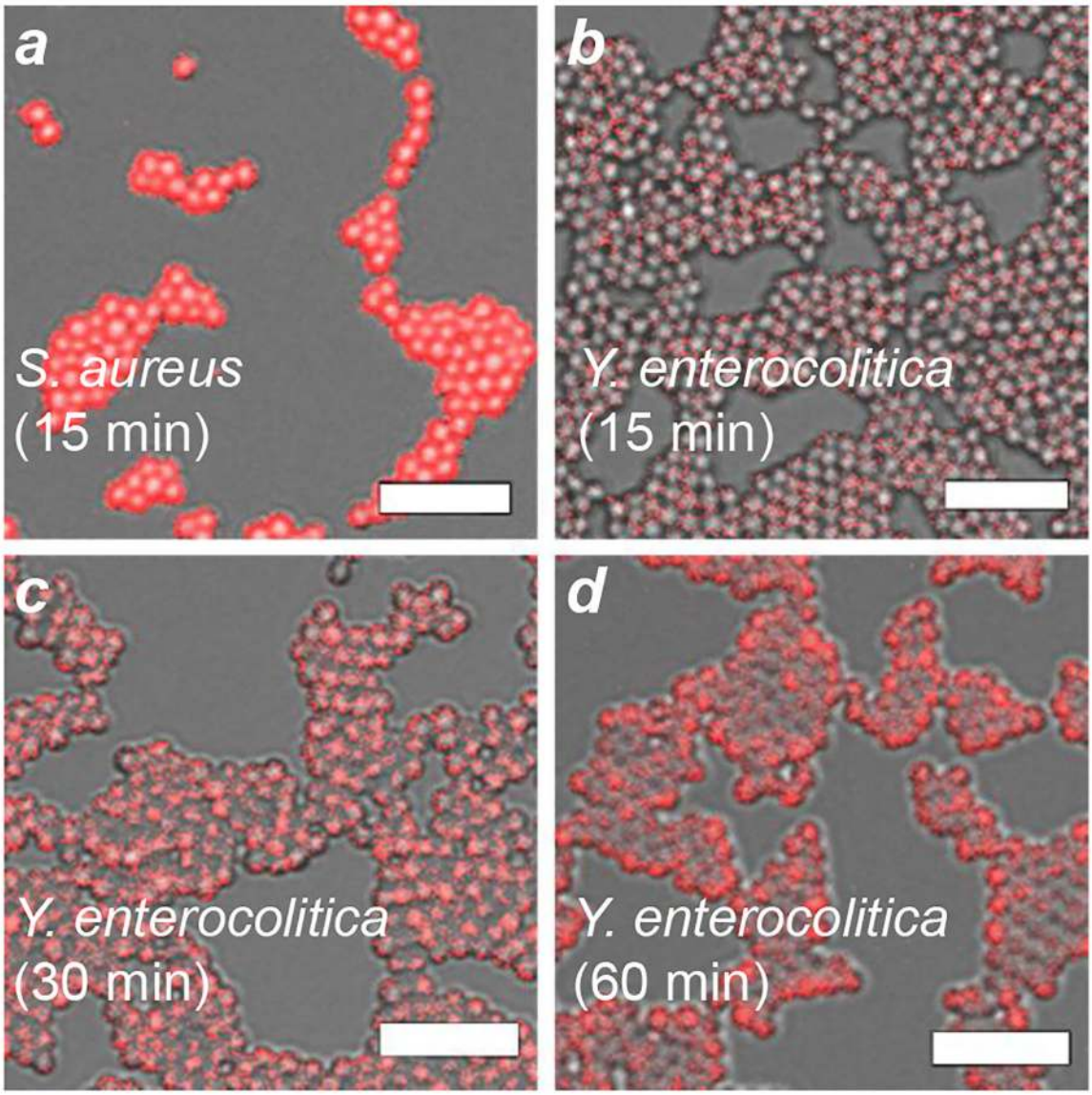

Figure 9.

Confocal fluorescence microscopy of Ga-PpIX uptake (bar = 5 μm). (*a*) *S. aureus* after 15 min incubation; (*b*–*d*) *Y. enterocolitica* (ovoid form) after 15, 30, and 60 min incubation.

Table 1.

aPDI activity of Ga-PpIX against various *S. aureus* strains

Light exposure (in seconds)[a]	Antimicrobial activity (3-log reduction)		Eradication (> 6-log reduction)
	conc. (μM)	aPDI potency[b]	conc. (μM)
S. aureus (PCI 1203; ATCC 10537)			
0 s (dark)	70		
10 s	0.03[c]	2400	0.24
30 s	<0.06[d]	--	0.12
MRSA (USA200), clinical isolate NRS 383			
0 s (dark)	36.3		
10 s	0.06	600	0.12
30 s	<0.06[d]	--	<0.06[d]
MRSA (USA500), clinical isolate NRS 385			
0 s (dark)	>145[e]		
10 s	0.09	>1600	0.47
30 s	<0.06[d]	--	<0.06[d]
MRSA (USA700), clinical isolate NRS 386			
0 s (dark)	>145[e]		
10 s	0.12	>1200	0.24
30 s	0.06	>2400	0.24
MRSA (USA800), clinical isolate NRS 387			
0 s (dark)	72.6		
10 s	0.06	1200	1.88
30 s	0.06	--	>0.24[f]

[a] Irradiated with 405-nm LED array (140 mW/cm^2 per well), with 10- and 30-s exposure times corresponding to 1.4 and 4.2 J/cm^2, respectively.

[b] Fold reduction in Ga-PpIX concentration, relative to dark toxicity (no light exposure).

[c] 3-log reduction within 1σ of experimental value.

[d] Lowest concentration tested at this fluence; > 3-log CFU/mL reduction.

[e] Highest concentration tested; < 3-log CFU/mL reduction.

[f] Highest concentration tested; < 6-log CFU/mL reduction.

Table 2.

Bacterial pathogens featured in Ga-PpIX uptake assay[a]

Bacteria, by classification	Culture conditions	Hemin acquisition proteins[c]
Type 1 (CSHR expressing)		
Bacillus anthracis (Ames 35)	Tryptic soy	Isd (C,E,X1,X2), BslK, Hal
Corynebacterium diphtheriae (5159)	Brain–heart infusion	HmuT, Hta (A,B)[48]
Staphylococcus aureus (PCI 1203)	Tryptic soy	Isd (A,B,C,E,H)
Staphylococcus epidermidis (ATCC 155)	Tryptic soy	Isd (A,B,C,E,H)
Streptococcus pneumoniae (CDC CS111)	Brain–heart infusion[b]	Unassigned[49,50]
Type 2 (hemophore producing)		
Acinetobacter baumannii (DSM 6974)	Nutrient broth	Unassigned[51,52,53]
Escherichia coli O157:H7 (CDC EDL 933)	Tryptic soy	ChuA, Hma, ShuA[54]
Klebsiella pneumoniae (S 389)	Nutrient broth	Unidentified[55]
Listeria monocytogenes (J0161)	Brain–heart infusion	HupC, Hbp2/SvpA
Haemophilus influenzae (AMC 36-A-5)	Gonococcal medium[b]	Hgp (A,B,C), Hup, HxuC
Pseudomonas aeruginosa (PAO1-LAC)	Luria–Bertani	Has (A,R), PhuR
Yersinia enterocolitica (WA-314)	Luria–Bertani	HemR
Type 3 (non-harvesters)		
Enterococcus faecium (VRE)	Brain–heart infusion	---
Salmonella enterica typhimurium (LT2)	Nutrient broth	---

[a] Details taken from Ref. 46 unless otherwise noted.

[b] 5% CO_2 atmosphere.

[c] Abbreviations: Bsl, *B. anthracis* S-layer; Chu, *E. coli* heme utilization; Hal, heme-acquisition leucine-rich; Has, heme acquisition system; Hbp, hemin binding protein; Hem, hemin receptor; Hgp, hemoglobin/haptoglobin binding protein; Hma, heme acquisition protein; Hmu, hemin uptake; Hta, hemin transport; Hup, heme uptake; Hxu, hemopexin uptake; Isd, iron-regulated surface determinant; Phu, *Pseudomonas* heme uptake; Shu, *Shigella* heme uptake; Svp, surface virulence-associated protein.